Journal of Medicinal Chemistry

Article

pubs.acs.org/jmc

Potent and Selective Aminopyrimidine-Based B-Raf Inhibitors with Favorable Physicochemical and Pharmacokinetic Properties

Simon Mathieu,[†] Stefan N. Gradl,[†] Li Ren,[‡] Zhaoyang Wen,[†] Ignacio Aliagas,[†] Janet Gunzner-Toste,[†] Wendy Lee,[†] Rebecca Pulk,[†] Guiling Zhao,[†] Bruno Alicke,[†] Jason W. Boggs,[†] Alex J. Buckmelter,[‡] Edna F. Choo,[†] Victoria Dinkel,[‡] Susan L. Gloor,[‡] Stephen E. Gould,[†] Joshua D. Hansen,[‡] Gregg Hastings,[‡] Georgia Hatzivassiliou,[†] Ellen R. Laird,[‡] David Moreno,[‡] Yingqing Ran,[†] Walter C. Voegtli,[‡] Steve Wenglowsky,[‡] Jonas Grina,[‡] and Joachim Rudolph*[,†]

[†]Genentech, Inc., 1 DNA Way, South San Francisco, California 94080-4990, United States

[‡]Array BioPharma, 3200 Walnut Street, Boulder, Colorado 80301, United States

Supporting Information

ABSTRACT: Recent clinical data provided proof-of-concept for selective B-Raf inhibitors in treatment of B-Raf^{V600E} mutant melanoma. Pyrazolopyridine-type B-Raf inhibitors previously described by the authors are potent and selective but exhibit low solubility requiring the use of amorphous dispersion-based formulation for achieving efficacious drug exposures. Through structure-based design, we discovered a new class of highly potent aminopyrimidine-based B-Raf inhibitors with improved solubility and pharmacokinetic profiles. The hinge binding moiety possesses a basic center imparting high solubility at gastric pH, addressing the dissolution limitation observed with our previous series. In our search for an optimal linker-hinge binding moiety system, amide-linked thieno[3,2-*d*]pyrimidine analogues **32** and **35** (G945), molecules with desirable physicochemical properties, emerged as lead compounds with strong efficacy in a B-Raf^{V600E} mutant mouse xenograft model. Synthesis, SAR, lead selection, and evaluation of key compounds in animal studies will be described.

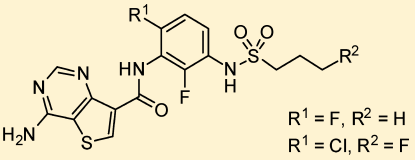

INTRODUCTION

The Raf enzyme family of protein kinases are members of the mitogen activated protein kinase (MAPK) cascade, a key pathway regulating cell proliferation, invasion, and survival.[1] Through specific mutations, members of this pathway can become constitutively active, leading to uncontrolled cell growth. A frequent aberration in human cancers is a substitution of a glutamic acid for valine at position 600 of the Raf family member B-Raf (V600E).[2] This mutation is particularly prominent in melanoma, where it occurs with a frequency of ∼60%.[3] On the basis of epidemiology and preclinical target validation, B-Raf has been recognized as an excellent target opportunity for cancer treatment. In fact, recent clinical data revealed a remarkable response of selective B-Raf inhibitors, and vemurafenib (PLX4032/RG7204, Plexxikon/Roche, **1**) recently received FDA approval for the treatment of melanoma.[4−6]

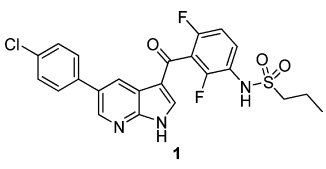

1

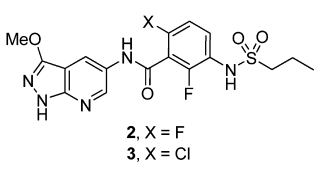

2, X = F
3, X = Cl

We recently reported the discovery of selective, orally bioavailable, and efficacious inhibitors of B-Raf^{V600E} that are based on a novel 3-methoxypyrazolopyridine hinge binding template.[7] Similarly to compounds previously reported by Plexxikon,[8] members of this series bind to the active conformation of the kinase (DFG-in) and induce a characteristic outward shift of the αC-helix. An essential structural factor of this shift is a sulfonamide alkyl tail residue opening a lipophilic pocket that accommodates said alkyl group, imparting high kinase selectivity.[8] Lead compounds **2** and **3** emerged as potent inhibitors and exhibited robust efficacy in B-Raf^{V600E} xenograft mouse models. However, the low solubility of **2** and **3** precluded the use of crystalline suspension formulations for covering the dose ranges required for efficacy and toxicology studies, and we resorted to amorphous spray-dried dispersion formulation.[7] Correspondingly, the sulfonamide-type clinical B-Raf inhibitor vemurafenib (**1**) was reformulated as micro-precipitated bulk powder (MBP) during phase 1 clinical studies to achieve efficacious drug exposure levels.[4,9] While amorphous dispersion formulations are increasingly being used for the development of drugs with low solubility,[10] traditional solid dosage using crystalline drug remains the most straightforward and preferred means of drug formulation. The study presented in this account describes our efforts in identifying inhibitors with improved physicochemical properties that would allow dosage as crystalline suspension.

Table 1 shows selected physicochemical data of compound **2**. The pK_a of its most basic center at the hinge portion is low, rendering this and related compounds largely unprotonated at

Received: January 4, 2012
Published: February 15, 2012

Table 1. Measured Physicochemical Properties of Compound 2

logP	pK_a[a] (most basic)	pK_a (most acidic)	mp [°C][a]	thermodynamic solubility [μg/mL], pH 1.2, 6.5, 7.4[b]
2.5	0.7	7.5	226	3/4/9

[a]Dissociation constant of the corresponding conjugated acid. [b]Data for highest melting crystalline polymorphs obtained in our hands.

gastric and intestinal tract pH values. In fact, compounds from this series are weak acids as a consequence of a sulfonamide −NH linked to an electron-deficient aromatic ring. Furthermore, melting points are typically high, indicating strong crystal lattice forces.[11] The combination of these factors likely accounts for the low solubility.

Focus of our strategy on improving solubility was the introduction of a basic center without adding significant molecular weight. We preferred to maintain the sulfonamide portion of the molecule due to its critical role in inferring kinase selectivity and instead attempted to make key modifications at the hinge binding portion of the molecule.

Two characteristic conformational features of the pyrazolopyridine series are a >60° torsion angle of the amide moiety relative to the 2,6-dihalo substituted central phenyl ring and a near coplanar arrangement of the amide moiety with the hinge binding heterocycle, a typical disposition of acylated anilines.[12] The central phenyl ring and the hinge binding heterocycle are in a near orthogonal spatial arrangement, and our goal was to mimic this arrangement with an alternative linker−hinge binder unit combination. This led us to the design of urea-linked pyrimidine scaffolds that are geometrically held in place via an intramolecular hydrogen bond (Figure 1). A similar pseudoring approach has been employed by others to replace a bicyclic core framework (e.g., pyrido[2,3-*d*]pyrimidin-7-one),[13,14] but to our knowledge, this approach had not been attempted to mimic an acylated aniline moiety.

We synthesized such urea-linked pyrimidine derivatives and found them indeed to have comparable activities to corresponding representatives of the first generation amide series; cocrystal structure analysis revealed a binding mode as hypothesized. Chemical stability problems prompted us to abandon the urea series and led us to the development of the related "reverse amide" linked 4-aminoquinazoline and 4-aminothienopyrimidine series, providing superior overall profiles. The following account will describe the development of these series and the synthesis and biological evaluation of selected compounds.

RESULTS AND DISCUSSION

Synthetic Chemistry. Representatives of the urea series were synthesized as described in Schemes 1, 2, and 3. The benzoic acid intermediate **6**[7] was converted into the corresponding amine **7** via a Curtius rearrangement reaction. Coupling with carbamate **5** furnished the urea derivative **8**, which was subsequently reacted with ammonia (**9a**) or primary amines **9b** and **9c** to form the target compounds **10**−**12**. The *N*-methyl urea analogue **15** was accessed via conversion of benzoic acid **6** into its isocyanate derivative, coupling with an appropriate methylaminopyrimidine **13**, and further transformation into the corresponding primary amine **15**. The pyrazolopyrimidine analogues **18** and **19** were obtained by a similar procedure, however the isolatable phenyl carbamate **16** was used for the formation of the urea bond.

The chemistry used to synthesize 4-aminoquinazoline or 4-aminothienopyrimidine core derivatives is described in Schemes 4 and 5. For the 4-aminoquinazoline core (Scheme 4), 2-aminoisophtalic acid **20** was condensed with formamide to afford benzoic acid intermediate **21**, which was bischlorinated and coupled with anilines **7a**−**7d**. The resulting chloroquinazolines **23a**−**d** were then treated with ammonia to obtain **24**−**27**. For the synthesis of 4-aminothieno[3,2-*d*]pyrimidine compounds (Scheme 5), precursor **28** was first brominated at the 7-position, followed by a carbonylation in methanol to generate the corresponding adduct **29**. Condensation with phosphorus oxychloride, followed by hydrolysis of the ester moiety, afforded acid **30**. Similar chemistry as used for scaffold A was performed to obtain **32**−**35**.

Lead Optimization and Structure−Activity Relationships. Following our design hypothesis explained in the introduction, we embarked on the synthesis of urea linker analogues, and, gratifyingly, prototype compounds, exemplified by **10** and **19**, were found to have higher potencies than their "amide series" counterparts **36** and **2** (Figure 3). To validate our design hypothesis, we attempted cocrystallization of selected urea analogues in B-Raf and succeeded with compound **12** (Figure 2). As hypothesized by molecular modeling, the 4-aminopyrimidine moiety forms similar hydrogen bond contacts with the hinge residue Cys532 as the previous lead compound **2**.[7] The intramolecular hydrogen bond between the distal linker urea −NH and the pyrimidine −N enforces a coplanar arrangement of this moiety, and analogous to the cocrystal structure of **2** in B-Raf, the hinge binding plane is oriented forming an torsion angle of >60° relative to the central 2,6-disubstituted phenyl ring (65.3°). Same as **2**, the −NH and $-SO_2$ portions of the sulfonamide are interacting with Asp594

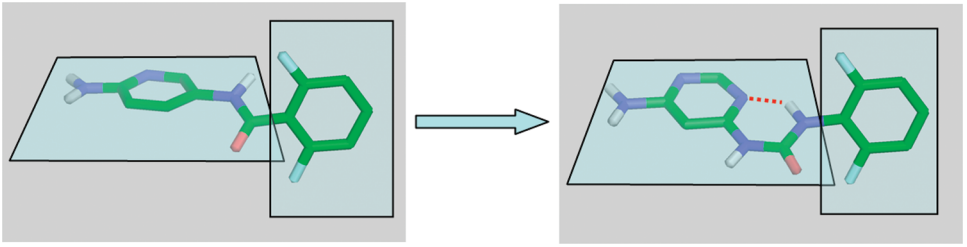

Figure 1. Structure models to illustrate the rescaffolding approach applied to the pyrazolopyridine series containing an amide linker unit (left). Rescaffolding using a urea linker constrained through an intramolecular hydrogen bond (right) maintains the near coplanarity of the linker−hinge binding plane and a near 90° torsion angle between this moiety and the connecting aryl unit. The red dotted line represents an intramolecular hydrogen bond.

dx.doi.org/10.1021/jm300016v | *J. Med. Chem.* 2012, 55, 2869−2881

Scheme 1. Synthesis of Aminopyrimidine Substituted Urea Analogues 10−12[a]

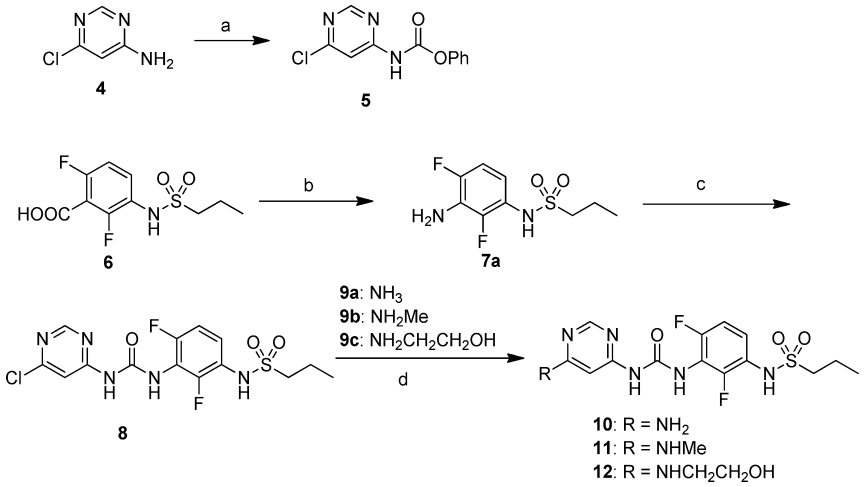

[a]Reagents and conditions: (a) phenylchloroformate, Cs_2CO_3, THF, 60 °C, 20 h, 37%; (b) diphenylphosphonic azide, NEt_3, THF, 80 °C, 55%; (c) **5**, DCE, 90 °C, 75%; (d) **9a**, **9b**, or **9c**, THF or DCE, 60−80 °C, 35−70%.

Scheme 2. Synthesis of Aminopyrimidine Substituted Methylurea Analogue 15[a]

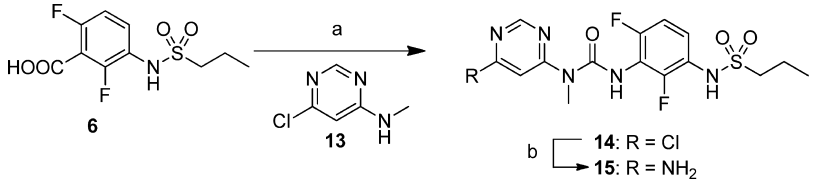

[a]Reagents and conditions: (a) diphenylphosphonic azide, NEt_3, THF, 80 °C, then **13**, 25%; (b) 7 M NH_3 in MeOH, rt, 40%.

Scheme 3. Synthesis of Pyrazolopyrimidine Substituted Urea Analogues 18 and 19[a]

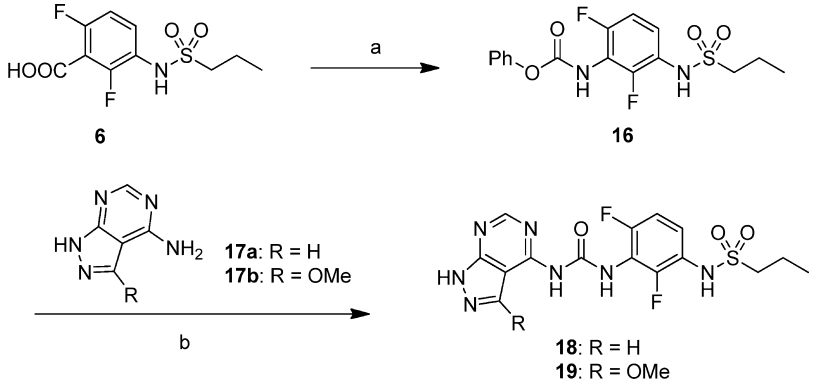

[a]Reagents and conditions: (a) diphenylphosphonic azide, NEt_3, dioxane, rt, then phenol, 100 °C, 5%; (b) **17a** or **17b**, DMSO, 80 °C, 5 h, 30−45%.

and Phe595-Gly596, respectively, and the propyl tail moiety fills a narrow lipophilic pocket.

Upon repeated cell assay testing of one of the most potent compounds in the urea series, **19**, we noticed a continuous loss of activity. Dedicated stability testings indeed revealed chemical degradation that was particularly rapid under acidic conditions. We believe that the intramolecular hydrogen bond is the prime reason for the observed instability; indeed related carbamoyl systems have been utilized as readily cleavable protecting groups of nucleobases.[15] This prompted us to abandon this series.[16]

We then explored structural alternatives that maintain the geometrical arrangement including the intramolecular hydrogen bond at the hinge binding region. One of our attempts was the replacement of the urea linker with a more stable amide-linked 4-aminoquinazoline core. To our delight, prototype "reverse amide" **24** displayed excellent enzyme and cellular potencies without any chemical stability issues at low pH.[16]

Our premise was the installation of a basic center to address the low solubility exhibited by the previous series, represented here by compounds **2** and **3**. As shown in Table 2, the aminoquinazoline moiety of **24** provides a basic center with a considerably higher pK_a (4.45, measured data)[17] compared to the parent compound **2** (pK_a = 0.7, measured data); consequently, the solubility of **24** at pH 1.2 was substantially increased, with a value of >1000 μg/mL (the solubility at pH 6.5 and 7.4 remained low at 1 μg/mL). As demonstrated later, this translated into benefits in in vivo studies.

dx.doi.org/10.1021/jm300016v | J. Med. Chem. 2012, 55, 2869−2881

Scheme 4. Synthesis of 4-Aminoquinazoline analogues 24−27[a]

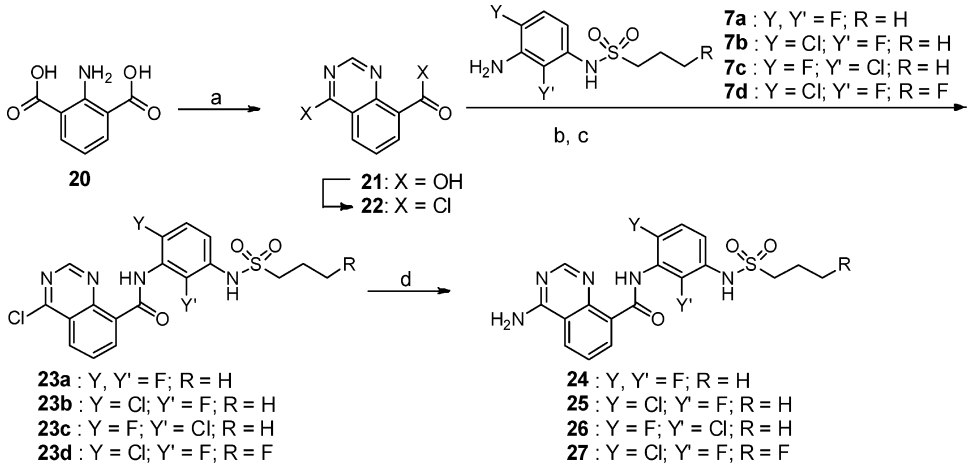

[a]Reagents and conditions: (a) formamide, formamidine acetate, 170 °C, 78%; (b) $SOCl_2$, DMF, 77%; (c) **7a−d**, pyridine, $MgSO_4$, $CHCl_3$, 22−76%; (d) 2 M NH_3/*i*-PrOH, 105 °C (microwave), 68−80%.

Scheme 5. Synthesis of 4-Aminothieno[3,2-*d*]pyrimidine Compounds 32−35[a]

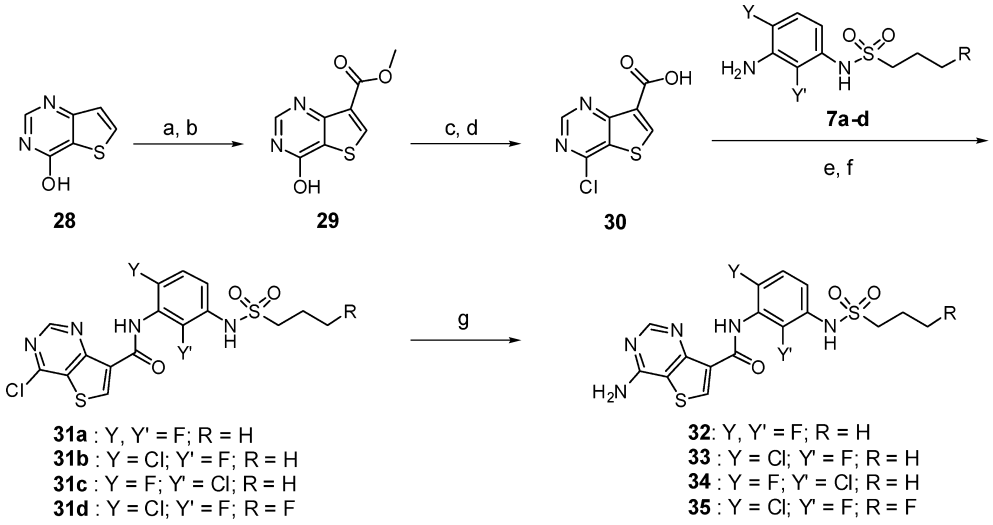

[a]Reagents and conditions: (a) Br_2, AcOH, 100 °C, 60%; (b) $PdCl_2$(dppf)·DCM, Et_3N, MeOH, CO (300 psi), 120 °C, 80%; (c) $POCl_3$, reflux, 96%; (d) LiOH, THF/H_2O, rt, 81%; (e) oxalyl chloride, DMF (cat.), THF; (f) **22a−d**, THF, rt, 61−100% for 2 steps; (g) 2 M NH_3/*i*-PrOH, 95 °C (thermal) or 110 °C (microwave), 61−89%.

Encouraged by the improved properties and potency of this new scaffold, we explored alternative ring systems. In these studies, 4-aminothieno[3,2-*d*]pyrimidine analogues, as represented by **32**, emerged as promising leads with comparable features to the aminoquinazolines. Compound **32** achieved potencies of 3 and 15 nM, respectively, in the biochemical and cellular assay (Table 3), and we succeeded in obtaining a cocrystal structure of this compound with B-Raf (Figure 4). Similar to the aminopyrimidine hydrogen bond contacts observed in the B-Raf cocrystal structure of the urea analogue **12**, the 4-aminothieno[3,2-*d*]pyrimidine moiety binds to the hinge residue Cys532. Furthermore, this cocrystal structure shared all the hallmark features observed in the cocrystal structure of **12**: (a) intramolecular hydrogen bond between the linker amide −NH and the pyrimidine −N enforcing a coplanar arrangement of this moiety, (b) hinge binding plane oriented in a near orthogonal fashion relative to the central 2,6-disubstituted phenyl ring (torsion angle of 82°), (c) −NH and $-SO_2$ portions of the sulfonamide interacting with Asp594 and Phe595-Gly596, respectively, (d) propyl tail moiety filling a narrow lipophilic pocket. In alignment with kinase selectivity profiles of other sulfonamide-type B-Raf inhibitors, **32** displayed high selectivity when tested against a large kinase panel, showing >100-fold selectivity for 268/273 tested kinases.[18]

Further SAR studies focused on the modification of the central ring and tail group, and selected data are shown in Table 3. Varying the halogen groups at the −2 and −6 positions on both scaffolds had subtle effects on enzyme and cellular potencies. Interestingly, compounds with X = Cl were consistently more potent than analogues with X = F in the biochemical assay but showed a noticeably larger shift from biochemical to cellular assay than the latter. We do not know if this is due to differences in cell permeability or other reasons. Placement of a fluorine at the end of the propyl tail group, as

dx.doi.org/10.1021/jm300016v | *J. Med. Chem.* 2012, 55, 2869−2881

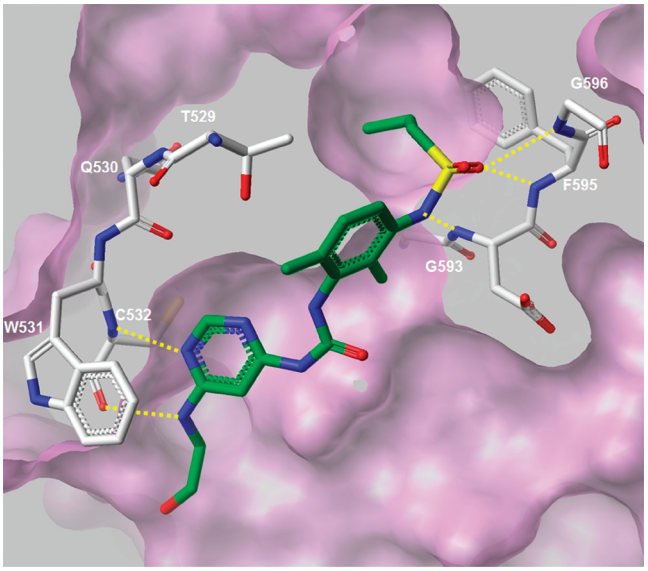

Figure 2. X-ray crystal structure of **12** (in green) in complex with B-Raf^{V600E}. The cleft surface is rendered in violet, and select residues are depicted in white. Hydrogen bonding interactions are illustrated with yellow dashed lines.

shown in a recent publication by us,[19] led to an increase in enzyme and cellular potencies in both scaffolds.

Profiling of Advanced Compounds. The favorable in vitro profiles prompted us to evaluate these compounds in vivo and selected in vivo as well as physicochemical data are shown in Table 4. Following IV dosing, all compounds exhibited very low clearance (CL) and volume of distribution (V_{ss}). Similar to previously reported B-Raf inhibitors with related chemotypes,[7] solubility at neutral pH for these and other compounds from this series is low. We believe that this is resulting from strong crystal lattice force, as suggested by high melting points. However, a dramatic difference to the previous series is the universally observed high solubility at pH 1.2, presumably resulting from the presence of the pyrimidine portion with increased pK_a. Previous B-Raf inhibitors with related chemotypes consistently produced low exposures when dosed as crystalline suspensions, likely as a result of a dissolution limitation.[20] Our hope was that the high solubility at gastric pH of the series described here would circumvent this limitation. All compounds shown in Table 4 were dosed as crystalline suspensions, and to our delight, oral bioavailability was consistently found to be high. As an example, compound **24** was also dosed in mice in solution and the resulting exposure was nearly matched by the exposure from dosing as crystalline suspension (AUC of 331 vs 290 μM·h). Among the two scaffolds investigated, we found the thieno[3,2-*d*]pyrimidine compounds to exhibit higher oral exposure than their quinazoline counterparts (Table 4). We account this to both the lower clearance and better thermodynamic solubility at neutral pH observed for the former series.

Extensive profiling of the compounds described above led us to select **35** (G945), a thieno[3,2-*d*]pyrimidine analogue, for advanced studies. **35** displays high overall kinase selectivity when tested in a large panel,[18] selectivity for inhibition of B-Raf^{V600E} vs WT B-Raf and WT C-Raf, and strong antiproliferative efficacy in B-Raf^{V600E} mutant cell lines (Table 5).

35 showed no significant CYP inhibition (CYP2C9 IC_{50} = 9 μM, IC_{50} of all other major CYPs > 25 μM) and no time-dependent CYP inhibition potential. Furthermore, it did not exhibit any significant activity in a broad receptor panel or hERG channel activity and was Ames-negative.

In vivo pharmacokinetic studies with compound **35** in rodents revealed extremely low IV clearance, very low volume of distribution, and excellent oral exposure after dosing as crystalline suspension (Table 6). Exposure increase was near dose-proportional in rat between 5 and 25 mg/kg and slightly less than proportional in mouse between 1 and 50 mg/kg. We do not believe that enterohepatic recirculation can explain the high rodent bioavailability, as clearance of compound **35** in both mice and rats was very low (less than 1% of hepatic blood flow), and metabolite levels will be low in turn. This is also supported by in vitro metabolite identification studies using rat and mouse hepatocytes which showed only minimal glucuronide metabolite formation.

The strong in vitro and in vivo profile of **35** led us to proceed to in vivo efficacy studies using the Colo205 xenograft mouse model. For benchmarking purposes, we dosed compound **2** in the same study. **35** was found to be both significantly more potent and efficacious in this model (Figure 5). We believe that this large difference results from both the higher biochemical activity and superior exposure of **35** compared to compound **2**.

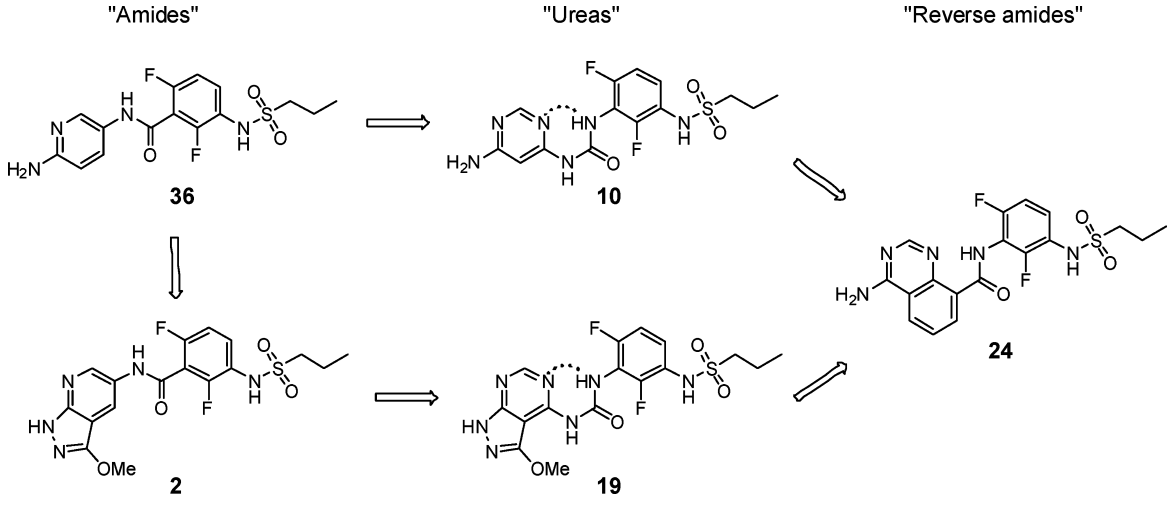

Figure 3. Conceptual path from the "amide" to the "reverse amide" series.

dx.doi.org/10.1021/jm300016v | *J. Med. Chem.* 2012, 55, 2869–2881

Table 2. Potencies (Biochemical and Cellular) and Selected Measured Properties of Compounds Shown in Figure 2 and Selected Compounds from the Urea Series

series	compd	B-Raf^{V600E} IC_{50} [nM][a,b]	pERK IC_{50} [nM][b,c]	measured pK_a[d,e]	solubility at pH 1.2 [μg/mL][g]
amides	**36**	917	2400		nd
	2	5	19	0.7	3
ureas	**10**	142	438		nd
	11	36	168		900
	12	64	3400		900
	15	83	240		nd
	18	5.6	88		7
	19	1.6	*f*	1.8	49
reverse amides	**24**	2	10	4.5	>1000

[a]Biochemical assay. [b]Averages of at least three measurements. [c]Cellular phosphorylation assay using B-Raf^{V600E} mutant Malme-3 M cell line. [d]p*K*a determination was performed at Sirius using the D-PAS technique. [e]Dissociation constants of the corresponding conjugated acids. [f]High variability among different measurements with EC_{50} values ranging from 2.6 nM to 1.4 μM (n = 14). [g]Thermodynamic solubility.

Table 3. Enzymatic and Cellular Potencies of 4-Aminoquinazoline and 4-Aminothieno[3,2-*d*]pyrimidine Scaffolds

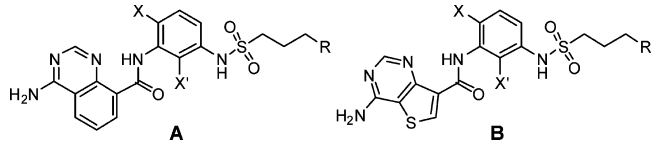

compd	scaffold (A/B)	X	X′	R	B-Raf^{V600E} IC_{50} (nM)[a,b]	pERK IC_{50} (nM)[b,c]
24	A	F	F	H	1.8	9.5
25	A	Cl	F	H	0.59	9.5
26	A	F	Cl	H	0.54	7.7
27	A	Cl	F	F	0.11	2.5
32	B	F	F	H	3.2	15
33	B	Cl	F	H	0.9	19
34	B	F	Cl	H	1.1	15
35	B	Cl	F	F	0.18	4.6

[a]Biochemical assay. [b]Averages of at least three measurements. [c]Cellular phosphorylation assay using B-Raf^{V600E} mutant Malme-3 M cell line.

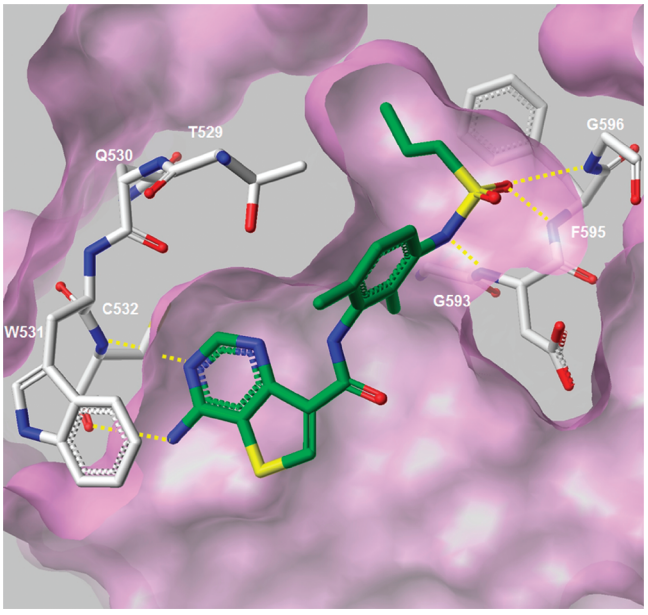

Figure 4. X-ray crystal structure of **32** (in green) in complex with B-Raf^{WT}. The cleft surface is rendered in violet, and select residues are depicted in white. Hydrogen-bonding interactions are illustrated with yellow dashed lines.

It is especially noteworthy that the efficacy profile of compound **35** was achieved via dosing as crystalline suspension, while compound **2** required formulation as amorphous dispersion. Even with the help of an amorphous dispersion formulation, compound **2** did not achieve >25% bioavailability at efficacious doses in mice,[7] which is in stark contrast to the high bioavailability observed with crystalline suspensions of compound **35**.

CONCLUSION

In conclusion, we discovered a potent and selective B-Raf inhibitor series that displays superior physicochemical characteristics compared to other sulfonamide-type B-Raf inhibitors previously reported by us. The key design step that led to the identification of this series was the replacement of the amide linked pyrazolopyridine hinge binding motif by a urea-linked aminopyrimidine system that is constrained by an intramolecular hydrogen bond and provides equivalent planarity of the hinge binding system compared to the previous series studies therein. Further development of this idea led to the identification of 4-aminoquinazoline and 4-aminothieno[3,2-*d*]pyrimidine linked through an amide moiety. pK_a of these systems is increased by several orders of magnitude affording very good solubility at gastric pH and resulting in high exposures after dosing as crystalline suspension, a key benefit over sulfonamide-type B-Raf inhibitors previously reported by

dx.doi.org/10.1021/jm300016v | *J. Med. Chem.* 2012, 55, 2869−2881

Table 4. Mouse Pharmacokinetic Profiles (IV, PO) and Selected Measured Physicochemical Data of Compounds 24, 32, and 35

compd	CL[a] [mL/min/kg]	V_{ss}[a] [L/kg]	30 mg/kg PO AUC[b] [μM·h]	30 mg/kg PO %F	mouse PPB (%)	thermodynamic solubility[c] pH 1.2/6.5[μg/mL]	mp (°C)	logP	pK_a[d] (most basic)
24	2.5	0.4	290	71	98.5	>1000/1	209	2.9	4.5
32	1.0	0.2	874	100	98.4	>1000/5	189	2.7	3.6
35	0.79	0.2	1680	>100	97.0	700/10	191	3.6	3.6

[a]IV dose: 2.5 mg/kg. [b]Compounds **24** and **32** dosed in 0.5% methylcellulose/0.2% Tween 80/99.3% water, compound **35** dosed in 20% HPBCD vehicle (20% hydroxypropyl-β-cyclodextrin/80% water). [c]Free-base form of highest melting crystalline polymorph found in our hands. [d]Dissociation constants of the corresponding conjugated acids.

Table 5. Biochemical Potencies of Compound 35 against B-Raf^{V600E} and Wild-Type Raf Isoforms and Antiproliferative Activities in Various Cell Lines

	Adjusted Inhibitor IC_{50} at 1 mM ATP [nM]
B-Raf^{V600E}	2
WT B-Raf	22 (11-fold)[a]
WT C-Raf	73 (152-fold)[a]
	Cellular Proliferation EC_{50} [nM]
A375-X1 (B-Raf^{V600E})[b]	2
Colo205 (B-Raf^{V600E})[b]	5
HT29 (B-Raf^{V600E}, EGFR^{high})[b]	24
RKO (B-Raf^{V600E}, EGFR^{high}, PTEN^{null})[b]	2310
H226 (wt)[b]	>10000

[a]Selectivity of B-Raf^{V600E} vs shown wild-type Raf isoforms. [b]Cell line genotype.

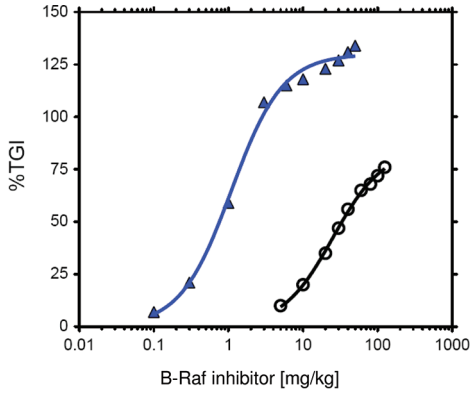

Compound	ED_{50} [mg/kg]	ED_{90} [mg/kg]	Max % TGI
35	1.1	6.2	130
2	25.2	139	76

Figure 5. Dose-ranging tumor growth inhibition studies in subcutaneous Colo205^{V600E} mouse xenograft model (qd × 21 d, po).

the authors. Compound **35** emerged as a highly potent lead compound with favorable overall properties and revealed both remarkable potency and efficacy in the B-Raf^{V600E} mutant Colo205 mouse xenograft in vivo model.

We did not detect adverse safety signals for compounds **32** and **35** in mouse efficacy studies, however, observations made in higher species precluded the advancement of these compounds, and we will report these data in due course.

EXPERIMENTAL SECTION

Chemical Syntheses. The reactions set forth below were conducted generally under a positive pressure of nitrogen or argon or with a drying tube in anhydrous solvents, and the reaction flasks were typically fitted with rubber septa for the introduction of substrates and reagents via syringe or cannula. Glassware was oven-dried and/or heat dried. All reagents and solvents were used without further purification unless otherwise stated. Reactions were monitored by either analytical TLC or analytical HPLC. Analytical TLC was performed using glass plates precoated with silica gel (manufacturer: EMD, Silica Gel 60 F254, 250 μm). Flash column chromatography was performed on an ISCO system having prepacked silica gel columns or on a Biotage model SP1 purification system running SPX software with prepacked silica gel columns and UV detection at 220 and 254 nm. LC-MS experiments were performed on an Agilent 1100 HPLC coupled with an Agilent MSD mass spectrometer using ESI as ionization source, employing two different methods (A and B). Solvent A was water with 0.05% TFA and solvent B acetonitrile with 0.05% TFA. Method A: An Agilent ZORBAX SB-C18 30 mm × 2.1 mm column was used with a 0.4 mL/min flow rate. The gradient steps consisted of 3−97% B over 7 min, holding 97% B for 1.5 min, followed by equilibration for 1.5 min. Method B: An Agilent ZORBAX SB-C18 100 mm × 3.0 mm column was used with a 0.7 mL/min flow rate. The gradient steps consisted of 2−98% solvent B over 25.5 min, holding 98% B for 2.5 min, followed by equilibration for 1.5 min. In both methods, peaks were detected by UV absorbance at 220 and 254 nm, and MS full scan was applied to all experiments. Melting points were recorded on an electrothermal melting point apparatus, model 9100.

Table 6. PK Profile of Compound 35 in Rodents[a]

	dose [mg/kg]							
	rat			mouse				
	1 mg/kg IV	5 mg/kg PO	25 mg/kg PO	2.5 mg/kg IV	1 mg/kg PO	10 mg/kg PO	30 mg/kg PO	50 mg/kg PO
CL [mL/min/kg]	0.19			0.79				
V_{ss} [L/kg]	0.14			0.12				
C_{max} (PO) [μM]		44.5	201		7.93	73	162	249
AUC (PO) [μM·h]		651	2970		84	867	1680	3249
%F		68	62		>100	>100	>100	>100

[a]Dosed as crystalline suspension, 20% HPBCD vehicle (20% hydroxypropyl-β-cyclodextrin/80% water).

dx.doi.org/10.1021/jm300016v | J. Med. Chem. 2012, 55, 2869−2881

^{1}H NMR spectra were recorded on a Varian Mercury (400 MHz) NMR spectrometer or on a Bruker AV III (400 or 500 MHz) spectrometer. Chemical shifts are expressed in parts per million (ppm, δ scale) using tetramethylsilane as the reference standard. When peak multiplicities are reported, the following abbreviations are used: s (singlet), d (doublet), t (triplet), q (quartet), m (multiplet), dd (doublet of doublet), dt (doublet of triplet), br (broad). Coupling constants are reported in hertz (Hz).

The purity of each compound that was synthesized and tested for biological activity was ≥95% via HPLC analysis.

Phenyl 6-Chloropyrimidin-4-ylcarbamate (5). A 5 mL reaction vial was charged with 6-chloropyrimidin-4-amine (**4**, 1043 mg, 8.05 mmol), phenylchloroformate (2.02 mL, 16.1 mmol), and cesium carbonate (5246 mg, 16.1 mmol) in THF. The reaction vessel was sealed and the mixture heated to 60 °C for 20 h. The solvent was removed to afford phenyl 6-chloropyrimidin-4-ylcarbamate as yellow solid (738 mg, 37%), which was used in the next step without further purification. ESI-MS: *m*/*z* 250.1 (M + 1).

***N*-(3-Amino-2,4-difluorophenyl)propane-1-sulfonamide (7a).** To a solution of 2,6-difluoro-3-(propylsulfonamido)benzoic acid[1] (4.078 g, 14.6 mmol) in THF (60 mL) was added triethylamine (4.68 mL, 33.59 mmol) and diphenylphosphonic azide (3.73 mL, 16.8 mmol). The reaction mixture was stirred at room temperature for 3 h and then warmed to 80 °C for 2 h. Water (10 mL) was added and the mixture stirred at 80 °C for 15 h. The reaction mixture was diluted with 300 mL of EtOAc, and the organic layer was washed with saturated aq $NaHCO_3$ solution and brine. The solvent was removed under reduced pressure and the residue purified silica gel column chromatography eluting with 30/70 EtOAc/hexane to obtain of *N*-(3-amino-2,4-difluorophenyl)propane-1-sulfonamide (2.03 g, 55%). ^{1}H NMR (400 MHz, DMSO-d_6) δ 9.32 (s, 1H), 6.90−6.80 (m, 1H), 6.51 (td, *J* = 8.7 Hz, 5.5 Hz, 1H), 5.28 (s, 2H), 3.05−2.96 (m, 2H), 1.82−1.64 (m, 2H), 1.01−0.90 (m, 3H). ESI-MS: *m*/*z* 251.1 (M + 1).

***N*-(3-Amino-4-chloro-2-fluorophenyl)propane-1-sulfonamide (7b).** Step A: A flame-dried flask equipped with a stir bar and rubber septum was charged with 4-chloro-2-fluoroaniline (5.00 g, 34.35 mmol) and anhydrous THF (170 mL). This solution was cooled to −78 °C, and *n*-BuLi (14.7 mL, 1.07 equiv of 2.5 M solution in hexanes) was then added over a 15 min period. This mixture was stirred at −78 °C for 20 min, and then a THF solution (25 mL) of 1,2-bis(chlorodimethylsilyl)ethane (7.76 g, 1.05 equiv) was added slowly (over a 10 min period) to the reaction mixture. The mixture was stirred for 1 h, and then 2.5 M *n*-BuLi in hexanes (15.1 mL, 1.1 equiv) was added slowly. After allowing the mixture to warm to room temperature for 1 h, the mixture was cooled to −78 °C. A third allotment of *n*-BuLi (15.66 mL, 1.14 equiv) was added slowly, and the mixture was stirred at −78 °C for 75 min. Benzyl chloroformate (7.40 g, 1.2 equiv) was then added slowly, and the mixture was stirred at −78 °C for 1 h. The cooling bath was then removed. The mixture was allowed to warm for 30 min and then quenched with water (70 mL) and concentrated HCl (25 mL). The mixture was allowed to continue to warm to room temperature and then extracted with EtOAc. The extracts were washed twice with a saturated $NaHCO_3$ solution, once with water, dried over sodium sulfate, and concentrated. The resulting residue was purified via silica gel column chromatography (30% ethyl acetate/hexane) to furnish benzyl 3-amino-6-chloro-2-fluorobenzoate (4.3 g, 45%) as an oil. ^{1}H NMR (DMSO-d_6, 400 MHz) δ 7.37−7.48 (m, 5H), 7.07 (dd, *J* = 8 Hz, 2 Hz, 1H), 6.87 (t, *J* = 8 Hz, 1H), 5.61 (br s, 2H), 5.40 (s, 2H).

Step B: Benzyl 3-amino-6-chloro-2-fluorobenzoate (4.3 g, 15.37 mmol) was dissolved in dry dichloromethane (270 mL). Triethylamine (5.36 mL, 2.5 equiv) was added, and the mixture was cooled to 0 °C. Propane-1-sulfonyl chloride (3.63 mL, 32.3 mmol, 2.1 equiv) was then added via a syringe, and a precipitate resulted. After the addition was complete, the mixture was allowed to warm to room temperature. The mixture was then diluted with dichloromethane (200 mL), washed with 2 M aqueous HCl (2 × 100 mL) and saturated aqueous $NaHCO_3$ solution, dried over sodium sulfate, and concentrated. The resulting residue was purified via silica gel column chromatography (40% ethyl acetate/hexane) to furnish benzyl 6-chloro-2-fluoro-3-(*N*-(propylsulfonyl)propylsulfonamido)benzoate (5.5 g, 72%) as an oil that slowly solidified upon standing. ^{1}H NMR ($CDCl_3$, 400 MHz) δ 7.28−7.45 (m, 7H), 5.42 (s, 2H), 3.58−3.66 (m, 2H), 3.43−3.52 (m, 2H), 1.08 (t, *J* = 8 Hz, 6H).

Step C: Benzyl 6-chloro-2-fluoro-3-(*N*-(propylsulfonyl)-propylsulfonamido) benzoate (5.4 g, 10.98 mmol) was dissolved in THF (100 mL) and 1 M aqueous KOH (100 mL). This mixture was heated at reflux for 16 h and then allowed to cool to room temperature. The mixture was then acidified to a pH of 2 with 2 M aqueous HCl and extracted with EtOAc (2×). The extracts were washed with water, dried over sodium sulfate, and concentrated to a solid that was triturated with hexanes/ether to give 6-chloro-2-fluoro-3-(propylsulfonamido)benzoic acid (2.2 g, 68%) as a solid. ^{1}H NMR (DMSO-d_6, 400 MHz) δ 9.93 (s, 1H), 7.49 (t, *J* = 8 Hz, 1H), 7.38 (dd, *J* = 8 Hz, 2 Hz, 1H), 3.11−3.16 (m, 2H), 1.68−1.78 (m, 2H), 0.97 (t, *J* = 8 Hz, 3H).

Step D: *N*-(3-Amino-4-chloro-2-fluorophenyl)propane-1-sulfonamide **7b** was made using a similar procedure as described for *N*-(3-Amino-2,4-difluorophenyl)propane-1-sulfonamide **7a**. ^{1}H NMR (500 MHz, DMSO-d_6) δ 9.54 (s, 1H), 7.02 (d, 1H), 6.58 (t, 1H), 5.50 (s, 2H), 3.09−2.95 (t, 2H), 1.81−1.64 (sx, 2H), 0.96 (t, 3H). ESI-MS: *m*/*z* 267.1 (M + 1).

***N*-(3-Amino-2-chloro-4-fluorophenyl)propane-1-sulfonamide (7c).** Step A: Into a 20 L 4-neck round flask was placed a solution of 2-chloro-4-fluorobenzenamine (1300 g, 8.82 mol, 1.00 equiv, 99%) in toluene (10 L), 4-methylbenzenesulfonic acid (3.1 g, 17.84 mmol, 99%), and hexane-2,5-dione (1222.5 g, 10.62 mol, 1.20 equiv, 99%). The resulting solution was heated to reflux for 1 h in an oil bath and cooled. The pH value of the solution was adjusted to 8 with sodium carbonate (1 mol/L). The resulting mixture was washed with 1 × 5000 mL of water and concentrated under vacuum. The crude product was purified by distillation and the fraction was collected at 140 °C to afford 1-(2-chloro-4-fluorophenyl)-2,5-dimethyl-1*H*-pyrrole (1700 g, 85%).

Step B: Into a 5000 mL 4-necked round-bottom flask purged and maintained with an inert atmosphere of nitrogen was placed a solution of 1-(2-chloro-4-fluorophenyl)-2,5-dimethyl-1*H*-pyrrole (390 g, 1.65 mol, 1.00 equiv, 95%) in THF (2000 mL). The reaction vessel was cooled to −78 °C. To the above reaction vessel was added *n*-BuLi (800 mL, 1.10 equiv, 2.5%) dropwise with stirring over 80 min and methyl carbonochloridate (215.5 g, 2.27 mol, 1.20 equiv, 99%) dropwise with stirring over 90 min. The reaction solution was further stirred for 60 min at −78 °C and quenched by the addition of 1000 mL of NH_4Cl/water. The resulting solution was extracted with 1500 mL of ethyl acetate. The organic layers were combined, washed with 1 × 1500 mL of water and 1 × 1500 mL of sodium chloride (aq), dried over anhydrous magnesium sulfate, and concentrated under vacuum to afford methyl 2-chloro-3-(2,5-dimethyl-1*H*-pyrrol-1-yl)-6-fluorobenzoate (crude, 566.7 g).

Step C: Into five 5000 mL 4-neck round-bottom flasks was placed a solution of methyl 2-chloro-3-(2,5-dimethyl-1*H*-pyrrol-1-yl)-6-fluorobenzoate (1500 g, 5.05 mol, 1.00 equiv, 95%) in ethanol/H_2O (7500/2500 mL), NH_2OH·HCl (5520 g, 79.20 mol, 15.00 equiv, 99%), and triethylamine (2140 g, 20.98 mol, 4.00 equiv, 99%). The resulting solution was heated at reflux for 18 h in an oil bath, cooled to room temperature, concentrated, and extracted with 3 × 3000 mL of ethyl acetate. The organic layers were combined, dried over anhydrous sodium sulfate, and concentrated under vacuum. The residue was purified using a silica gel column eluting with PE:EA (20:1−10:1) to afford methyl 3-amino-2-chloro-6-fluorobenzoate (980 g, 95%).

Step D: Into four 5000 mL 4-neck round-bottom flasks was placed a solution of methyl 3-amino-2-chloro-6-fluorobenzoate (980 g, 4.76 mol, 1.00 equiv, 99%) in dichloromethane (8000 mL). Triethylamine (1454 g, 14.25 mol, 3.00 equiv, 99%) was added dropwise with stirring at 0 °C over 80 min followed by the addition of propane-1-sulfonyl chloride (1725 g, 11.94 mol, 2.50 equiv, 99%). The resulting solution was stirred at room temperature for 2 h and diluted with 1000 mL of water. The organic layer was washed with 1 × 1000 mL of hydrogen chloride and 1 × 1000 mL of water, dried over sodium sulfate, and

concentrated to afford methyl 2-chloro-6-fluoro-3-(propylsulfonamido)benzoate as a brown solid (1500 g, 97%).

Step E: Into a 10000 mL 4-necked round-bottom flask was placed a solution of methyl 2-chloro-6-fluoro-3-(propylsulfonamido)benzoate (1500 g, 4.61 mol, 1.00 equiv, 95%) in THF/H_2O (3000/3000 mL) and potassium hydroxide (1000 g, 17.68 mol, 4.50 equiv, 99%). The resulting solution was refluxed for 2 h, cooled to room temperature, and extracted with 3 × 2000 mL of ethyl acetate. The aqueous layers were combined, and the pH was adjusted to 2 with hydrogen chloride (2 mol/L). The resulting solution was extracted with 2 × 3000 mL of dichloromethane. The organic layers were combined, dried over anhydrous sodium sulfate, and concentrated to afford 2-chloro-6-fluoro-3-(propylsulfonamido)benzoic acid (517.5 g, 37%). ^{1}H NMR (400 MHz, $CDCl_3$): δ 1.058−1.096 (m, J = 15.2 Hz, 3H), 1.856−1.933 (m, 2H), 3.073−3.112 (m, 2H), 6.811 (1H, s), 7.156−7.199 (d, J = 17.2 Hz, 1H), 7.827−7.863 (d, J = 14.4 Hz, 1H). ESI-MS: m/z 296.0 (M + 1).

Step F: *N*-(3-Amino-2-chloro-4-fluorophenyl)propane-1-sulfonamide **7c** was made using a similar procedure as described for *N*-(3-amino-2,4-difluorophenyl)propane-1-sulfonamide **7a**. ^{1}H NMR (400 MHz, DMSO-d_6) δ 9.20 (s, 1H), 7.28−6.99 (m, 1H), 6.63 (td, J = 8.7 Hz, 5.5 Hz, 1H), 5.45 (s, 2H), 3.07−2.99 (m, 2H), 1.88−1.69 (m, 2H), 1.03− 0.95 (m, 3H). ESI-MS: m/z 267.1 (M + 1).

***N*-(3-Amino-4-chloro-2-fluorophenyl)-3-fluoropropane-1-sulfonamide (7d).** Step A: Into a 5000 mL 4-necked round-bottom flask was placed a solution of benzyl 3-amino-6-chloro-2-fluorobenzoate (200 g, 714.29 mmol, 1.00 equiv) (previously described in the synthesis of **7b**) in dichloromethane (2000 mL) and triethylamine (216 g, 2.14 mol, 3.00 equiv) followed by the addition of a solution of 3-fluoropropane-1-sulfonyl chloride (227 g, 1.42 mol, 2.00 equiv) in dichloromethane (300 mL) dropwise with stirring at about 8 °C over 60 min. After stirring at room temperature for 3 h, the resulting mixture was washed with 500 mL of 5N HCl and 2 × 500 mL of water. The organic layer was dried over anhydrous sodium sulfate and concentrated under vacuum to afford benzyl 6-chloro-2-fluoro-3-(3-fluoro-*N*-(3-fluoropropylsulfonyl)propylsulfonamido)benzoate (360 g, 91%) as a brown oil.

Step B: A solution of benzyl 6-chloro-2-fluoro-3-(3-fluoro-*N*-(3-fluoropropylsulfonyl)propylsulfonamido)benzoate (360 g, 647.73 mmol, 1.00 equiv, 95%) in THF (1800 mL) and KOH (2M, 1680 mL) was stirred at 50 °C for 12 h. The resulting mixture was cooled and concentrated under vacuum to remove most of THF. The residual solution was washed with 3 × 500 mL of EtOAc. The aqueous layer was adjusted to pH 2−3 with HCl (6M). The resulting solution was extracted with 4 × 500 mL of ethyl acetate. The combined organic layers were dried over anhydrous sodium sulfate and concentrated under vacuum to afford 6-chloro-2-fluoro-3-(3-fluoropropylsulfonamido)benzoic acid (190 g, 89%). ^{1}H NMR (400 MHz, DMSO-d_6) δ 9.65 (br s, 1H), 7.03 (m, 1H), 6.58 (m, 1H), 4.59 (m, 1H), 4.47 (m, 1H), 3.18 (m, 2H), 2.22−2.02 (m, 2H). ESI-MS: m/z 312.1 [M-1].

Step C: Into a 3000 mL 3-necked round-bottom flask was placed a solution of 6-chloro-2-fluoro-3-(3-fluoropropylsulfonamido)benzoic acid (190 g, 574.8 mmol, 1.00 equiv, 95%) in *N*,*N*-dimethylformamide (1500 mL) and triethylamine (184 g, 1.82 mol, 3.0 equiv) followed by the addition of diphenylphosphoryl azide (250 g, 909.1 mmol, 1.50 equiv) dropwise with stirring at 5 °C over 10 min. After stirring at 5 °C for 2 h, water (500 mL) was added to the reaction mixture. The resulting solution was stirred at 80 °C in an oil bath for an additional 2 h, cooled, and diluted with 2000 mL of EtOAc. The organic layer was washed with 4 × 1000 mL of brine, dried over anhydrous sodium sulfate, and concentrated under vacuum. The residue was purified via silica gel column chromatography eluting with ethyl acetate/petroleum ether (1:3) to afford *N*-(3-amino-4-chloro-2-fluorophenyl)-3-fluoropropane-1-sulfonamide (76 g, 46%) as a white solid. ^{1}H NMR (400 MHz, $CDCl_3$) δ 7.04−7.06 (m, 1H), 6.91−6.87 (t, 1H), 6.39 (s, 1H), 4.62−4.59 (t, 1H), 4.40−4.57 (t, 1H), 4.15 (br s, 2H), 3.27−3.24 (t, 2H), 2.30−2.16 (m, 2H). ESI-MS: m/z 283.0 [M − 1].

***N*-(3-(3-(6-Chloropyrimidin-4-yl)ureido)-2,4-difluorophenyl)propane-1-sulfonamide (8).** Phenyl 6-chloropyrimidin-4-ylcarbamate (204 mg, 0.817 mmol) and *N*-(3-amino-2,4-difluorophenyl)-propane-1-sulfonamide (225 mg, 0.899 mmol) were taken up in 1,2-dichloroethane (3 mL, 41 mmol). The reaction mixture was heated at 90 °C for 15 h, cooled to room temperature, and concentrated under reduced pressure. Purification via silica gel column chromatography (eluent: ethylacetate/hexane 1:1) afforded *N*-(3-(3-(6-chloropyrimidin-4-yl)ureido)-2,4-difluorophenyl)propane-1-sulfonamide (250 mg, 75%). ^{1}H NMR (400 MHz, DMSO-d_6) δ 10.50−10.24 (s, 1H), 9.28−9.12 (s, 1H), 8.73−8.64 (d, J = 1.0 Hz, 1H), 7.78−7.71 (d, J = 1.0 Hz, 1H), 7.38−7.28 (td, J = 8.8, 5.6 Hz, 1H), 7.20−7.07 (td, J = 9.3, 1.8 Hz, 1H), 6.45−6.50 (m, 1H), 3.06−2.99 (m, 2H), 1.79−1.68 (m, 2H), 1.01−0.92 (t, J = 7.4 Hz, 3H). ESI-MS: m/z 406.0 (M + 1).

***N*-(3-(3-(6-Aminopyrimidin-4-yl)ureido)-2,4-difluorophenyl)propane-1-sulfonamide (10).** *N*-(3-(3-(6-Chloropyrimidin-4-yl)-ureido)-2,4-difluorophenyl)propane-1-sulfonamide (**8**, 66 mg, 0.16 mmol) was added to a mixture of 7 M ammonia in methanol (2 mL). The reaction stirred at 80 °C overnight. After removal of the solvent under reduced pressure, the crude product was purified by reverse phase HPLC, affording 20 mg (35%) of the title compound. HPLC RT = 3.11 min (method A). ESI-MS: m/z 387.1 (M + 1). ^{1}H NMR (400 MHz, DMSO-d_6) 9.92 (s, 1H), 9.53 (s, 1H), 8.35 (s, 1H), 8.11 (s, 1H), 7.28 (dd, J = 14.7, 8.8, 1H), 7.08 (dd, J = 20.0, 9.8, 1H), 6.81 (s, 2H), 6.41 (s, 1H), 3.07−2.94 (m, 2H), 1.81−1.64 (m, 2H), 0.96 (t, J = 7.4, 3H).

***N*-(2,4-Difluoro-3-(3-(6-(methylamino)pyrimidin-4-yl)-ureido)phenyl)propane-1-sulfonamide (11).** *N*-(3-(3-(6-Chloropyrimidin-4-yl)ureido)-2,4-difluorophenyl)propane-1-sulfonamide (**8**, 30 mg, 0.07 mmol) was added to a solution of 2 M methylamine in THF (2 mL), and the reaction mixture was stirred at 80 °C overnight. The organic solvent was removed under reduced pressure and the crude product purified by reverse phase HPLC affording 20 mg (70%) of the title compound. HPLC RT = 3.20 min (method A). ESI-MS: m/z 401.1 (M + 1). ^{1}H NMR (400 MHz, DMSO-d_6) 9.83 (br s, 2H), 9.48 (s, 1H), 8.18 (d, J = 6.8, 1H), 7.35−7.24 (m, 2H), 7.16 (t, J = 9.4, 1H), 6.45 (s, 1H), 3.14−2.98 (m, 2H), 2.72 (m, 3H), 1.87−1.63 (m, 2H), 0.99 (t, J = 7.4, 3H).

***N*-(2,4-Difluoro-3-(3-(6-(2-hydroxyethyl-amino)pyrimidin-4-yl)ureido)phenyl)propane-1-sulfonamide (12).** *N*-(3-(3-(6-Chloropyrimidin-4-yl)ureido)-2,4-difluorophenyl)propane-1-sulfonamide (**8**, 30 mg, 0.07 mmol) and ethanolamine (40 μL, 0.7 mmol) were dissolved in dichloroethane (0.6 mL). *N*,*N*-Diisopropyl-ethylamine (100 μL, 0.7 mmol) was added followed by stirring at 60 °C overnight. After removal of the solvent under reduced pressure, the crude product was purified by silica gel chromatography eluting with 0−100% hexane/EtOAc to afford 15 mg (50%) of the title compound. HPLC RT = 3.10 min (method A). ESI-MS: m/z 431.1(M + 1). ^{1}H NMR (400 MHz, DMSO-d_6) 9.83 (s, 1H), 9.49 (s, 1H), 8.19 (d, J = 15.6, 1H), 7.56−7.21 (m, 2H), 7.14 (t, J = 8.7, 1H), 6.52 (d, J = 24.6, 1H), 4.71 (m, 2H), 3.48 (m, 2H), 3.15−2.93 (m, 2H), 1.83−1.63 (m, 2H), 0.97 (t, J = 7.4, 3H).

6-Chloro-*N*-methylpyrimidin-4-amine (13). 4,6-Dichloropyrimidine (978 mg, 6.56 mmol) was taken up in isopropyl alcohol (10 mL, 131 mmol) followed by cooling to 0−5 °C. A solution of 33% methylamine in ethanol (1.768 mL, 13.2 mmol) was added, and the reaction mixture was stirred for 15 h. The mixture was concentrated under reduced pressure and suspended in water. The title compound was obtained after filtration and drying in vacuo (772 mg, 82%). ESI-MS: m/z 144.1 (M + 1). ^{1}H NMR (400 MHz, DMSO-d_6) δ 8.27 (s, 1H), 7.65 (s, 1H), 6.50 (s, 1H), 2.99−2.67 (m, 3H).

***N*-(3-(3-(6-Chloropyrimidin-4-yl)-3-methylureido)-2,4-difluorophenyl)propane-1-sulfonamide (14).** 2,6-Difluoro-3-(propylsulfonamido)benzoic acid (**6**, 1.05 g, 3.76 mmol) was taken up in THF (20 mL, 0.2 mol), and triethylamine (1.2 mL, 8.64 mmol) was added in. Then, diphenylphosphonic azide (930.9 μL, 4.32 mmol) was added, and the mixture was stirred at room temperature for 2 h. The mixture was then heated at 80 °C for 1 h, and 6-chloro-*N*-methylpyrimidin-4-amine (674 mg, 4.70 mmol) was added. After stirring at 80 °C overnight, the reaction mixture was diluted with EtOAc (300 mL) and washed subsequently with saturated aqueous Na_2CO_3 solution and brine (50 mL each). The organic phase was

concentrated under reduced pressure and the residue purified via silica gel chromatography (eluent: 0−50% ethylacetate in hexane) to obtain 365 mg (25%) of the title compound. ESI-MS: m/z 420.1 (M + 1).

***N*-(3-(3-(6-Aminopyrimidin-4-yl)-3-methylureido)-2,4-difluorophenyl)propane-1-sulfonamide (15).** *N*-(3-(3-(6-Chloropyrimidin-4-yl)-3-methylureido)-2,4-difluorophenyl)propane-1-sulfonamide (**14**, 26 mg, 0.062 mmol) was added to a 7 M solution of ammonia in methanol (1 mL, 6.7 mmol). The reaction mixture was stirred at room temperature overnight, concentrated under reduced pressure, and purified via reverse phase HPLC to obtain 15 mg (40%) of the title compound. HPLC RT = 3.37 min (method A). ESI-MS: m/z 401.1 (M + 1). ^{1}H NMR (400 MHz, DMSO-d_6) 12.10 (s, 1H), 9.80 (s, 1H), 8.22 (s, 1H), 7.27 (dd, J = 14.6, 8.8, 1H), 7.07 (t, J = 9.2, 1H), 6.99 (s, 2H), 6.14 (s, 1H), 3.31 (s, 3H), 3.06−2.88 (m, 2H), 1.83−1.60 (m, 2H), 0.96 (t, J = 7.4, 3H).

Phenyl 2,6-Difluoro-3-(propylsulfonamido)-phenylcarbamate (16). 2,6-Difluoro-3-(propylsulfonamido)benzoic acid[7] (4 g, 14 mmol) was dissolved in 1,4-dioxane (100 mL), and triethylamine (2.2 mL, 16 mmol) and diphenylphosphonic azide (3.4 mL, 16 mmol) were added. The reaction mixture was stirred at room temperature for 3 h and then added dropwise to a solution of phenol (15 g, 160 mmol) in 1,4-dioxane (100 mL) at 100 °C. The mixture was stirred at 100 °C for 3 h and then cooled to room temperature. Silica was added, and the mixture was concentrated. Purification via flash chromatography (gradient elution, solvent: 0−30% ethyl acetate in heptanes) yielded the title compound (2.9 g, 55%). ^{1}H NMR (400 MHz, DMSO-d_6) δ 9.85 (s, 1H), 9.68 (s, 1H), 7.49−7.30 (m, 3H), 7.30−7.11 (m, 4H), 3.11−3.03 (m, 2H), 1.83−1.61 (m, 2H), 0.96 (t, J = 7.4, 3H).

3-Methoxy-1*H*-pyrazolo[3,4-*d*]pyrimidin-4-amine (17b). To a mixture of tetracyanoethylene (300 g, 2.34 mol) and urea (47.7 g, 0.79 mol) at rt was added methanol (1 L). The reaction mixture was heated at 35 °C for 20 min, cooled to room temperature, and diluted with diethyl ether (4 L). The mixture was cooled at −78 °C for 3 h, filtered, washed with cold ether (400 mL), and dried in vacuo to give 2-(dimethoxymethylene)malononitrile (200 g, 62%) as a white solid, which was used directly in the next step.

To a mixture of 2-(dimethoxymethylene)malononitrile (200 g, 1.45 mol) in H_2O (2.7 L) at rt was added hydrazine monohydrate (78 mL, 1.63 mol). The reaction mixture was stirred for 14 h, filtered, washed with H_2O (400 mL), and dried in vacuo to afford 5-amino-3-methoxy-1*H*-pyrazole-4-carbonitrile (140 g, 70%) as a light-yellow solid. ^{1}H NMR (400 MHz, DMSO-d_6) δ 11.04 (bs, 1 H), 6.35 (bs, 2 H), 3.76 (s, 3 H).

A mixture of 5-amino-3-methoxy-1*H*-pyrazole-4-carbonitrile (140 g, 1.01 mol) and formamidine acetate (140 g, 1.34 mol) was heated at 145 °C for 1 h, cooled to rt, and diluted with H_2O (1.2 L). The mixture was vigorously stirred for 2 h and filtered. The solid was washed with methanol (400 mL) and dried in vacuo to afford 3-methoxy-1*H*-pyrazolo[3,4-*d*]pyrimidin-4-amine (105 g, 64%) as a brown solid. ^{1}H NMR (400 MHz, DMSO-d_6) δ 12.31 (bs, 1 H), 8.07 (s, 1 H), 7.48 (bs, 1 H), 6.63 (bs, 1H), 3.94 (s, 3 H).

***N*-(2,4-Difluoro-3-(3-(3-methoxy-1*H*-pyrazolo[3,4-*d*]-pyrimidin-4-yl)ureido)phenyl)propane-1-sulfonamide (19).** The mixture of phenyl 2,6-difluoro-3-(propylsulfonamido)-phenylcarbamate (638 mg, 1.72 mmol) and 3-methoxy-1*H*-pyrazolo-[3,4-*d*]pyrimidin-4-amine (313 mg, 1.89 mmol) was suspended in dimethyl sulfoxide (2 mL). The reaction mixture was stirred at 80 °C for 5 h. Purification by HPLC afforded 540 mg (30%) of the title compound. HPLC RT = 4.17 min (method A). ESI-MS: m/z 442.0 (M + 1). ^{1}H NMR (400 MHz, DMSO-d_6) 13.09 (s, 1H), 11.10 (s, 1H), 9.81 (s, 1H), 8.52 (d, J = 22.0, 2H), 7.35 (dd, J = 14.1, 8.3, 1H), 7.17 (t, J = 9.1, 1H), 4.05 (s, 3H), 3.05 (m, 2H), 1.86−1.65 (m, 2H), 0.97 (t, J = 7.4, 3H).

***N*-(3-(3-1*H*-Pyrazolo[3,4-*d*]pyrimidin-4-ylureido)-2,4-difluorophenyl)propane-1-sulfonamide (18).** The title compound was synthesized using an analogous procedure as described for compound **19**. HPLC RT = 3.63 min (method A). ESI-MS: m/z 412.0 (M + 1). ^{1}H NMR (400 MHz, DMSO-d_6) 13.99 (s, 1H), 11.13 (s, 1H), 11.03 (s, 1H), 9.68 (s, 1H), 8.59 (s, 1H), 8.54 (s, 1H), 7.37 (dd, J = 14.6, 8.8, 1H), 7.20 (t, J = 9.5, 1H), 3.16−3.01 (m, 2H), 1.84−1.67 (m, 2H), 0.98 (t, J = 7.4, 3H).

4-Hydroxyquinazoline-8-carboxylic Acid (21). A 10 L reactor was charged with 2-aminoisophthalic acid **20** (600 g, 3.3 mol) and formamidine acetate (1035 g, 9.9 mol, 3.0 equiv). After stirring for 25 min, formamide (132 mL, 3.3 mol) was added. The mixture was heated at 170 °C with a sand bath and continuously stirred with a heavy duty overhead mechanical stirrer for 5 h. HPLC analysis indicated no presence of 2-aminoisophthalic acid. The temperature was lowered to 80 °C. Water (5 L) was slowly added to the reactor. The resulting suspension was heated under reflux for 1 h. The reaction mixture was then cooled to room temperature and filtered. The filter cake was washed with water (2 × 2 L) and MeOH (2 × 2 L). The filter cake was dried in an oven over 40 °C for 17 h. The first crop of the final product was obtained (384 g). To the previously obtained filtrate, concentrated HCl was added and the pH adjusted to 0.2. The mixture was filtered, and the filter cake washed with water (500 mL). Drying in the oven at 40 °C for 16 h yielded a second crop of the product which was combined with the first crop. Both product crops were combined to afford 4-hydroxyquinazoline-8-carboxylic acid (500 g, 87%). ^{1}H NMR (400 MHz, DMSO-d_6) δ 8.51 (s, 1H), 8.45 (dd, J = 7.6, 1.6 Hz, 1H), 8.35 (dd, J = 7.9, 1.6 Hz, 1H), 7.68 (t, J = 7.8 Hz, 1H).

4-Chloroquinazoline-8-carbonyl Chloride (22). 4-Hydroxyquinazoline-8-carboxylic acid **21** (2.50 g, 13.1 mmol) was suspended in thionyl chloride (40 mL), and DMF (0.20 mL, 2.63 mmol) was added. The reaction mixture was heated at reflux for 2 h, and the remaining undissolved solid was filtered off. The filtrate was concentrated in vacuo and the residue redissolved in chloroform and reconcentrated in vacuo. The same process was repeated twice with toluene. The obtained solid was triturated with heptane and filtered to afford 4-chloroquinazoline-8-carbonyl chloride (2.30 g, 77%). ^{1}H NMR (400 MHz, DMSO-d_6) δ 8.56 (s, 1H), 8.48 (dd, J = 7.6, 1.6 Hz, 1H), 8.39 (dd, J = 7.9, 1.6 Hz, 1H), 7.71 (t, J = 7.8 Hz, 1H). m/z (ESI-MS) (M − (2 Cl) + (2 -OMe) + 1) = 219.2.

4-Amino-quinazoline-8-carboxylic Acid [2,6-Difluoro-3-(propane-1-sulfonylamino)-phenyl]-amide (24). Step A: To a solution of *N*-(3-amino-2,4-difluorophenyl)propane-1-sulfonamide **7a** (170 mg, 0.679 mmol) in chloroform (3 mL) was added magnesium sulfate (150 mg) and pyridine (0.16 mL, 2.04 mmol). A suspension of 4-chloroquinazoline-8-carbonyl chloride (0.20 g, 0.88 mmol) in chloroform (4 mL) was then added at room temperature. The reaction mixture was heated at 60 °C for 1 h, and the magnesium sulfate was removed by filtration. The filtrate was diluted with dichloromethane and washed with a saturated solution of $NaHCO_3$. The aqueous layer was extracted twice with dichloromethane and the combined organic layers dried with sodium sulfate, filtered, and concentrated in vacuo. The crude product was purified by flash chromatography eluting with 10−20% EtOAc/DCM to afford 4-chloro-*N*-(2,6-difluoro-3-(propylsulfonamido)phenyl)quinazoline-8-carboxamide **23a** (145 mg, 48%). Step B: In a microwave vessel, 4-chloro-*N*-(2,6-difluoro-3-(propylsulfonamido)phenyl)quinazoline-8-carboxamide **23a** (0.08 g, 0.18 mmol) was dissolved in a 2 M ammonia solution in isopropyl alcohol (4 mL) and heated in a microwave reactor at 105 °C for 15 min. The reaction mixture was concentrated in vacuo and the crude product then purified by SFC (or reverse phase HPLC) to afford the title compound (55 mg, 71%) as a solid. HPLC RT = 7.90 min (method B). ESI-MS: m/z 422.1 (M + 1). ^{1}H NMR (400 MHz, DMSO-d_6) δ 13.25 (s, 1H), 9.67 (s, 1H), 8.65 (d, J = 6.6 Hz, 1H), 8.57 (s, 1H), 8.53 (d, J = 8.1, 1H), 8.33 (s, 2H), 7.68 (t, J = 7.8 Hz, 1H), 7.37 (dd, J = 14.4, 8.6 Hz, 1H), 7.22 (t, J = 8.6 Hz, 1H), 3.14−3.01 (m, 2H), 1.82−1.69 (m, 2H), 0.98 (t, J = 7.4 Hz, 3H).

4-Amino-quinazoline-8-carboxylic Acid [6-Chloro-2-fluoro-3-(propane-1-sulfonylamino)-phenyl]-amide (25). Step A: 4-Chloro-*N*-(6-chloro-2-fluoro-3-(propylsulfonamido)phenyl)-quinazoline-8-carboxamide **23b** was made using a similar procedure as described for 4-chloro-*N*-(2,6-difluoro-3-(propylsulfonamido)phenyl)-quinazoline-8-carboxamide **23a**. Step B: 4-Amino-quinazoline-8-carboxylic acid [6-chloro-2-fluoro-3-(propane-1-sulfonylamino)-phenyl]-amide **25** was made using a similar procedure as described for 4-

amino-quinazoline-8-carboxylic acid [2,6-difluoro-3-(propane-1-sulfonylamino)-phenyl]-amide **24**. HPLC RT = 9.07 min (method B). ESI-MS: m/z 438.0 (M + 1). ^{1}H NMR (400 MHz, DMSO-d_6) δ 13.47 (s, 1H), 9.90 (s, 1H), 8.65 (dd, J = 7.5, 1.4 Hz, 1H), 8.58 (s, 1H), 8.53 (dd, J = 8.3, 1.4 Hz, 1H), 8.43 (s, 1H), 8.26 (s, 1H), 7.69 (t, J = 7.9 Hz, 1H), 7.47−7.36 (m, 2H), 3.16−3.08 (m, 2H), 1.75 (sx, J = 7.4 Hz, 2H), 0.97 (t, J = 7.4 Hz, 3H).

4-Amino-quinazoline-8-carboxylic Acid [2-Chloro-6-fluoro-3-(propane-1-sulfonylamino)-phenyl]-amide (26). Step A: 4-Chloro-*N*-(2-chloro-6-fluoro-3-(propylsulfonamido)phenyl)-quinazoline-8-carboxamide **23c** was made using a similar procedure as described for 4-chloro-*N*-(2,6-difluoro-3-(propylsulfonamido)phenyl)-quinazoline-8-carboxamide **23a**. Step B: 4-Amino-quinazoline-8-carboxylic acid [2-chloro-6-fluoro-3-(propane-1-sulfonylamino)-phenyl]-amide **26** was made using a similar procedure as described for 4-amino-quinazoline-8-carboxylic acid [2,6-difluoro-3-(propane-1-sulfonylamino)-phenyl]-amide **24**. HPLC RT = 8.00 min (method B). ESI-MS: m/z 438.0 (M + 1). ^{1}H NMR (400 MHz, DMSO-d_6) δ 13.25 (s, 1H), 9.68 (s, 1H), 8.69−8.61 (m, 1H), 8.57 (s, 1H), 8.56−8.49 (m, 1H), 8.32 (s, 2H), 7.68 (t, J = 7.8 Hz, 1H), 7.37 (td, J = 8.8, 5.7 Hz, 1H), 7.22 (t, J = 8.7 Hz, 1H), 3.15−3.03 (m, 2H), 1.84−1.68 (m, 2H), 1.04 (d, J = 6.1 Hz, 1H), 1.02−0.93 (m, 3H).

4-Amino-quinazoline-8-carboxylic Acid [6-Chloro-2-fluoro-3-(3-fluoro-propane-1-sulfonylamino)-phenyl]-amide (27). Step A: 4-Chloro-*N*-(6-chloro-2-fluoro-3-(3-fluoropropylsulfonamido)phenyl)quinazoline-8-carboxamide **23d** was made using a similar procedure as described for 4-chloro-*N*-(2,6-difluoro-3-(propylsulfonamido)phenyl)quinazoline-8-carboxamide **23a**. Step B: 4-Amino-quinazoline-8-carboxylic acid [6-chloro-2-fluoro-3-(3-fluoro-propane-1-sulfonylamino)-phenyl]-amide **27** was made using a similar procedure as described for 4-amino-quinazoline-8-carboxylic acid [2,6-difluoro-3-(propane-1-sulfonylamino)-phenyl]-amide **24**. HPLC RT = 3.40 min (method A). ESI-MS: m/z 456.1, 458.1 (M + 1). ^{1}H NMR (400 MHz, DMSO-d_6) δ 13.46 (s, 1H), 9.98 (s, 1H), 8.68−8.62 (m, 1H), 8.58 (s, 1H), 8.55−8.50 (m, 1H), 8.30 (br s, 2H), 7.68 (t, J = 7.8 Hz, 1H), 7.47−7.37 (m, 2H), 4.60 (t, J = 6.0 Hz, 1H), 4.48 (t, J = 6.0 Hz. 1H), 3.27−3.21 (m, 2H), 2.19−2.04 (m, 2H).

Methyl 4-Hydroxythieno[3,2-*d*]pyrimidine-7-carboxylate (29). Step A: To a solution of 3*H*-thieno[3,2-*d*]pyrimid-4-one **28** (25 g, 164 mmol) in acetic acid (200 mL) was added bromine (26 mL) dropwise. The reaction mixture was heated at 100 °C for 8 h. The resulting suspension was cooled to room temperature, poured into water, and neutralized with solid sodium bicarbonate. The solid product was collected by vacuum filtration to yield 7-bromo-3*H*-thieno[3,2-*d*]pyrimid-4-one (21.4 g, 60%) as a solid. ^{1}H NMR (500 MHz, DMSO-d_6) δ 12.75 (s, 1H), 8.38 (s, 1H), 8.27 (s, 1H). Step B: 7-Bromo-3*H*-thieno[3,2-*d*]pyrimid-4-one (10.0 g, 40.7 mmol), [1,1′-bis-(diphenyl-phosphino)ferrocene]dichloropalladium(II) complex with dichloromethane (1:1) (830.5 mg, 1.017 mmol), triethylamine (28.35 mL, 203.4 mmol), and methanol (80 mL) were combined in an autoclave fitted with a large stir bar. The mixture was purged with nitrogen for 5 min. The vessel was placed under an atmosphere of carbon monoxide (300 psi) and heated to 120 °C for 3 h. The vessel was cooled to room temperature, and the reaction mixture was filtered. The collected solids were washed with methanol (250 mL). The solids were air-dried to give the title compound (6.8 g, 80%). ^{1}H NMR (400 MHz, DMSO-d_6) δ 12.74 (s, 1H), 8.90 (s, 1H), 8.27 (s, 1H), 3.89 (s, 3H).

4-Chlorothieno[3,2-*d*]pyrimidine-7-carboxylic Acid (30). Step A: Methyl 4-hydroxythieno[3,2-*d*]pyrimidine-7-carboxylate **29** (6.8 g, 31 mmol) was dissolved in phosphoryl chloride (100 mL, 1000 mmol) and heated to reflux for 2 h. The mixture was stirred at room temperature overnight. The phosphoryl chloride was distilled off, and the solids were neutralized with ice and sodium bicarbonate. The resulting suspension was filtered to give a solid, which was triturated with anhydrous ether. The resulting suspension was filtered to yield methyl 4-chlorothieno[3,2-*d*]pyrimidine-7-carboxylate as a solid (6.76 g, 96%). ^{1}H NMR (400 MHz, DMSO-d_6) δ 9.30 (s, 1H), 9.17 (s, 1H), 3.91 (s, 3H). Step B: To a solution of methyl 4-chlorothieno[3,2-*d*]pyrimidine-7-carboxylate (2.00 g, 8.75 mmol) in THF (60 mL) and water (20 mL) was added lithium hydroxide monohydrate (0.59 g, 14.0 mmol). The reaction mixture was stirred at room temperature for 2 h, after which the volatiles were concentrated in vacuo. Water was added and a solid was obtain after filtration, which was rinsed with water and dried on a lyophilizer to afford 4-chlorothieno[3,2-*d*]pyrimidine-7-carboxylic acid (1.56 g, 81%). ^{1}H NMR (500 MHz, DMSO-d_6) δ 8.98 (s, 1H), 8.69 (s, 1H).

4-Amino-thieno[3,2-*d*]pyrimidine-7-carboxylic Acid [6-Chloro-2-fluoro-3-(propane-1-sulfonylamino)-phenyl]-amide (33). Step A: To a solution of 4-chlorothieno[3,2-*d*]pyrimidine-7-carboxylic acid **30** (0.93 g, 4.31 mmol) in THF (45 mL) at 0 °C was added oxalyl chloride (730 μL, 8.63 mmol) followed by DMF (14.5 μL, 0.19 mmol). The reaction mixture was stirred at room temperature for 75 min and then concentrated in vacuo to give crude 4-chlorothieno[3,2-*d*]pyrimidine-7-carbonyl chloride, which was used directly in the next step. Step B: Crude 4-chlorothieno[3,2-*d*]pyrimidine-7-carbonyl chloride was dissolved in THF (40 mL), and *N*-(3-amino-4-chloro-2-fluorophenyl)propane-1-sulfonamide **7b** (1.00 g, 3.75 mmol) was added. The reaction mixture was stirred at 55 °C for 90 min, cooled to room temperature, and diluted with dichloromethane and a saturated aqueous solution of $NaHCO_3$. The layers were separated and the aqueous layer extracted with dichloromethane (2×). The combined organic layers were dried over sodium sulfate, filtered, and concentrated in vacuo. The crude product was purified by flash chromatography to afford 4-chloro-*N*-(6-chloro-2-fluoro-3-(propylsulfonamido)phenyl)thieno[3,2-*d*]-pyrimidine-7-carboxamide **31b** (1.65 g, 95%). ^{1}H NMR (500 MHz, DMSO-d_6) δ 10.72 (s, 1H), 9.88 (s, 1H), 9.36 (s, 1H), 9.26 (s, 1H), 7.47−7.42 (m, 2H), 3.19−3.07 (m, 2H), 1.79−1.71 (m, 2H), 0.98 (t, J = 7.4 Hz, 3H). ESI-MS: m/z 463.0, 465.0 (M + 1). Step C: A sealed tube was charged with 4-chloro-*N*-(6-chloro-2-fluoro-3-(propylsulfonamido)phenyl)thieno[3,2-*d*]pyrimidine-7-carboxamide **31b** (1.65 g, 3.56 mmol), and a 2 M ammonia solution in isopropyl alcohol (27 mL) was added. The reaction mixture was heated at 95 °C for 24 h and then concentrated in vacuo. The crude product was triturated with 2% *i*-PrOH/water solution (crude could also be purified by reverse phase HPLC) to afford the title compound (1.41 g, 89%). HPLC RT = 9.69 min (method B). ESI-MS: m/z 444.0 (M + 1). ^{1}H NMR (400 MHz, DMSO-d_6) δ 11.47 (s, 1H), 9.90 (s, 1H), 8.98 (s, 1H), 8.55 (s, 1H), 7.97 (s, 2H), 7.49−7.36 (m, 2H), 3.18−3.07 (m, 2H), 1.81−1.67 (m, 2H), 0.97 (t, J = 7.4 Hz, 3H).

4-Amino-thieno[3,2-*d*]pyrimidine-7-carboxylic Acid [2,6-Difluoro-3-(propane-1-sulfonylamino)-phenyl]-amide (32). Step A: 4-Chloro-*N*-(2,6-difluoro-3-(propylsulfonamido)phenyl)thieno-[3,2-*d*]pyrimidine-7-carboxamide **31a** was made using a similar procedure as described for 4-chloro-*N*-(6-chloro-2-fluoro-3-(propylsulfonamido)phenyl)thieno[3,2-*d*]pyrimidine-7-carboxamide **31b**. Step B: 4-Amino-thieno[3,2-*d*]pyrimidine-7-carboxylic acid [2,6-difluoro-3-(propane-1-sulfonylamino)-phenyl]-amide **32** was made using a similar procedure as described for 4-amino-thieno[3,2-*d*]pyrimidine-7-carboxylic acid [6-chloro-2-fluoro-3-(propane-1-sulfonylamino)-phenyl]-amide **33**. HPLC RT = 8.72 min (method B). ESI-MS: m/z 428.0 (M + 1). ^{1}H NMR (400 MHz, DMSO-d_6) δ 11.49 (s, 1H), 9.62 (s, 1H), 8.98 (s, 1H), 8.56 (s, 1H), 7.97 (s, 2H), 7.47 (dd, J = 9.1, 5.3 Hz, 1H), 7.39 (t, J = 9.1 Hz, 1H), 3.18−3.09 (m, 2H), 1.77 (dd, J = 15.2, 7.5 Hz, 2H), 0.99 (t, J = 7.4 Hz, 3H).

4-Amino-thieno[3,2-*d*]pyrimidine-7-carboxylic Acid [2-Chloro-6-fluoro-3-(propane-1-sulfonylamino)-phenyl]-amide (34). Step A: 4-Chloro-*N*-(2-chloro-6-fluoro-3-(propylsulfonamido)-phenyl)thieno[3,2-*d*]pyrimidine-7-carboxamide **31c** was made using a similar procedure as described for 4-chloro-*N*-(6-chloro-2-fluoro-3-(propylsulfonamido)phenyl)thieno[3,2-*d*]pyrimidine-7-carboxamide **31b**. Step B: 4-Amino-thieno[3,2-*d*]pyrimidine-7-carboxylic acid [2-chloro-6-fluoro-3-(propane-1-sulfonylamino)-phenyl]-amide **34** was made using a similar procedure as described for 4-amino-thieno[3,2-*d*]pyrimidine-7-carboxylic acid [6-chloro-2-fluoro-3-(propane-1-sulfonylamino)-phenyl]-amide **33**. HPLC RT = 9.06 min (method B). ESI-MS: m/z 444.0 (M + 1). ^{1}H NMR (400 MHz, DMSO-d_6) δ 11.49 (s, 1H), 9.62 (s, 1H), 8.98 (s, 1H), 8.56 (s, 1H), 7.97 (s, 2H), 7.47 (dd, J

dx.doi.org/10.1021/jm300016v | J. Med. Chem. 2012, 55, 2869−2881

= 9.1, 5.3 Hz, 1H), 7.39 (t, J = 9.1 Hz, 1H), 3.18−3.09 (m, 2H), 1.77 (dd, J = 15.2, 7.5 Hz, 2H), 0.99 (t, J = 7.4 Hz, 3H).

4-Amino-thieno[3,2-*d*]pyrimidine-7-carboxylic Acid [6-Chloro-2-fluoro-3-(3-fluoro-propane-1-sulfonylamino)-phenyl]-amide (35). Step A: 4-Chloro-*N*-(6-chloro-2-fluoro-3-(3-fluoropropylsulfonamido)phenyl)thieno[3,2-*d*]pyrimidine-7-carboxamide **31d** was made using a similar procedure as described for 4-chloro-*N*-(6-chloro-2-fluoro-3-(propylsulfonamido)phenyl)thieno[3,2-*d*]pyrimidine-7-carboxamide **31b**. Step B: 4-Amino-thieno[3,2-*d*]-pyrimidine-7-carboxylic acid [6-chloro-2-fluoro-3-(3-fluoro-propane-1-sulfonylamino)-phenyl]-amide **35** was made using a similar procedure as described for 4-Amino-thieno[3,2-*d*]pyrimidine-7-carboxylic acid [6-chloro-2-fluoro-3-(propane-1-sulfonylamino)-phenyl]-amide **33**. HPLC RT = 9.06 min (method B). ESI-MS: m/z 462.1, 464.1 (M + 1). ^{1}H NMR (400 MHz, DMSO-d_6) δ 11.49 (br s, 1H), 10.03 (br s, 1H), 8.97 (s, 1H), 8.55 (s, 1H), 7.96 (br s, 2H), 7.43 (m, 2H), 4.61 (m, 1H), 4.49 (m, 1H), 3.25 (m, 2H), 2.17−2.04 (m, 2H).

■ ASSOCIATED CONTENT

Ⓢ Supporting Information

Kinase activity profiles of compounds **32** and **35**. Biological assay and solubility assay information. Chemical stability data for **19** and **24**. Protein expression and purification of B-Raf and B-Raf^{V600E} protein constructs for crystallography. Crystal structure determination of B-Raf complex with compound **12** and **32**, respectively. Colo205 xenograft efficacy study details for compound **35** and **2**. This material is available free of charge via the Internet at http://pubs.acs.org.

■ AUTHOR INFORMATION

Corresponding Author

*Phone: 650 467 8867. E-mail: rudolph.joachim@gene.com.

Notes

The authors declare no competing financial interest.

■ ACKNOWLEDGMENTS

We thank Laura Afflerbaugh and Jane Kuo for their drug formulation support.

■ ABBREVIATIONS USED

Ac, acetyl; ACN, acetonitrile; ADME, absorption, distribution, metabolism, and excretion; aq, aqueous; AUC, area under curve; CHAPS, 3-[(3-cholamidopropyl)dimethylammonio]-1-propanesulfonate; CL, clearance; C_{max}, maximal concentration; CYP, cytochrome P-450; d, day; DCE, dichloroethane; DCM, dichloromethane; DFG, sequence of the three amino acids aspartic acid-phenylalanine-glycine; DMF, *N*,*N*-dimethylformamide; DMSO, dimethylsulfoxide; D-PAS, dip probe absorption spectroscopy; EC_{50}, half-maximal effective concentration; ED_{50}, half-maximal effective dose; ED_{90}, dose associated with 90% of the maximum effectiveness; ESI, electrospray ionization; %*F*, oral bioavailability; equiv, equivalent; FDA, Food and Drug Administration; mp, melting point; HBSS, Hank's balanced salt solution; hERG, human ether-a-go-go related gene; HFBA, heptafluorobutyric acid; HPLC, high performance liquid chromatography; HPMCAS, hydroxypropylmethylcellulose acetate succinate; IC_{50}, half-maximal inhibitory concentration; h, hour; IPA, isopropyl alcohol; IV, intravenous administration; LC, liquid chromatography; MAPK, mitogen activated protein kinase; MS, mass spectrometry; MW, microwave; MW, molecular weight; $PdCl_2(dppf)\cdot DCM$, 1,1′-bis-(diphenylphosphino)ferrocene-palladium(II)dichloride dichloromethane complex; $Pd_2(dba)_3$, tris-(dibenzylideneacetone)dipalladium(0); PEG, polyethylene glycol; Ph, phenyl; PIPES, piperazine-*N*,*N*′-bis(2-ethanesulfonic acid); PK, pharmacokinetics; PO, oral administration; PPB, plasma protein binding; qd, dosing once daily; rmsd, root-mean-square deviation; rt, room temperature; RT, retention time; SAR, structure−activity relationship; TCEP, tris(2-carboxyethyl)phosphine; TGI, tumor growth inhibition; THF, tetrahydrofuran; V_{ss}, steady-state volume of distribution; TLC, thin-layer chromatography; UPLC, ultraperformance liquid chromatography; WT, wild-type

■ REFERENCES

(1) Peyssonnaux, C.; Eychene, A. The Raf/MEK/ERK pathway: new concepts of activation. *Biol. Cell* **2001**, *93*, 53−62.

(2) Wan, P. T.; Garnett, M. J.; Roe, S. M.; Lee, S.; Niculescu-Duvaz, D.; Good, V. M.; Jones, C. M.; Marshall, C. J.; Springer, C. J.; Barford, D.; Marais, R. Mechanism of activation of the RAF-ERK signaling pathway by oncogenic mutations of B-RAF. *Cell* **2004**, *116*, 855−867.

(3) Cohen, Y.; Xing, M.; Mambo, E.; Guo, Z.; Wu, G.; Trink, B.; Beller, U.; Westra, W. H.; Ladenson, P. W.; Sidransky, D. BRAF mutation in papillary thyroid carcinoma. *J. Natl. Cancer Inst.* **2003**, *95*, 625−627.

(4) Bollag, G.; Hirth, P.; Tsai, J.; Zhang, J.; Ibrahim, P. N.; Cho, H.; Spevak, W.; Zhang, C.; Zhang, Y.; Habets, G.; Burton, E. A.; Wong, B.; Tsang, G.; West, B. L.; Powell, B.; Shellooe, R.; Marimuthu, A.; Nguyen, H.; Zhang, K. Y. J.; Artis, D. R.; Schlessinger, J.; Su, F.; Higgins, B.; Iyer, R.; D'Andrea, K.; Koehler, A.; Stumm, M.; Lin, P. S.; Lee, R. J.; Grippo, J.; Puzanov, I.; Kim, K. B.; Ribas, A.; McArthur, G. A.; Sosman, J. A.; Chapman, P. B.; Flaherty, K. T.; Xu, X.; Nathanson, K. L.; Nolop, K. Clinical efficacy of a RAF inhibitor needs broad target blockade in BRAF-mutant melanoma. *Nature* **2010**, *467*, 596−599.

(5) Flaherty, K. T.; Puzanov, I.; Kim, K. B.; Ribas, A.; McArthur, G. A.; Sosman, J. A.; O'Dwyer, P. J.; Lee, R. J.; Grippo, J. F.; Nolop, K.; Chapman, P. B. Inhibition of Mutated, Activated BRAF in Metastatic Melanoma. *N. Engl. J. Med.* **2010**, *363*, 809−819.

(6) Another selective B-Raf inhibitor in advanced clinical studies is dabrafenib (GSK2118436, GlaxoSmithKline) Kefford, R.; Arkenau, H. T.; Brown, M. P.; Millward, M.; Infante, J. R.; Long, G. V.; Ouellet, D.; Curtis, M.; Lebowitz, P. F.; Falchook, G. S. Phase I/II study of GSK2118436, a selective inhibitor of oncogenic mutant BRAF kinase, in patients with metastatic melanoma and other solid tumors. *J. Clin. Oncol.* **2010**, *28* (15 Suppl (May 20 Supplement)), 8503.

(7) Wenglowsky, S.; Ren, L.; Ahrendt, K. A.; Laird, E. R.; Aliagas, I.; Alicke, B.; Buckmelter, A. J.; Choo, E. F.; Dinkel, V.; Feng, B.; Gloor, S. L.; Gould, S. E.; Gross, S.; Gunzner-Toste, J.; Hansen, J. D.; Hatzivassiliou, G.; Liu, B.; Malesky, K.; Mathieu, S.; Newhouse, B.; Raddatz, N. J.; Ran, Y.; Rana, S.; Randolph, N.; Risom, T.; Rudolph, J.; Savage, S.; Selby, L. T.; Shrag, M.; Song, K.; Sturgis, H. L.; Voegtli, W. C.; Wen, Z.; Willis, B. S.; Woessner, R. D.; Wu, W.-I.; Young, W. B.; Grina, J. Pyrazolopyridine Inhibitors of B-RafV600E. Part 1: The Development of Selective, Orally Bioavailable, and Efficacious Inhibitors. *ACS Med. Chem. Lett.* **2011**, *2*, 342−347.

(8) Tsai, J.; Lee, J. T.; Wang, W.; Zhang, J.; Cho, H.; Mamo, S.; Bremer, R.; Gillette, S.; Kong, J.; Haass, N. K.; Sproesser, K.; Li, L.; Smalley, K. S. M.; Fong, D.; Zhu, Y.-L.; Marimuthu, A.; Nguyen, H.; Lam, B.; Liu, J.; Cheung, I.; Rice, J.; Suzuki, Y.; Luu, C.; Settachatgul, C.; Shellooe, R.; Cantwell, J.; Kim, S.-H.; Schlessinger, J.; Zhang, K. Y. J.; West, B. L.; Powell, B.; Habets, G.; Zhang, C.; Ibrahim, P. N.; Hirth, P.; Artis, D. R.; Herlyn, M.; Bollag, G. Discovery of a selective inhibitor of oncogenic B-Raf kinase with potent antimelanoma activity. *Proc. Natl. Acad. Sci. U.S.A.* **2008**, *105*, 3041−3046.

(9) Flaherty, K.; Puzanov, I.; Sosman, J.; Kim, K.; Ribas, A.; McArthur, G.; Lee, R. J.; Grippo, J. F.; Nolop, K.; Chapman, P. Phase I study of PLX4032: proof of concept for V600E BRAF mutation as a therapeutic target in human cancer. *J. Clin. Oncol.* **2009**, *27* (15S (May 20 Supplement)), 9000.

(10) Vasconcelos, T.; Sarmento, B.; Costa, P. Solid dispersions as strategy to improve oral bioavailability of poor water soluble drugs. *Drug Discovery Today* **2007**, *12*, 1068−1075.
(11) A single X-ray structure analysis of compound **2** revealed hydrogen bond linked head-to-tail dimers involving both the pyrazolopyridine and the sulfonamide moiety Wenglowsky, S.; Moreno, D.; Rudolph, J.; Ran, Y.; Ahrendt, K. A.; Arrigo, A.; Colson, B.; Gloor, S. L.; Hastings, G. Pyrazolopyridine inhibitors of B-Raf^{V600E}. Part 3: An increase in aqueous solubility via the disruption of crystal packing. *Bioorg. Med. Chem. Lett.* **2012**, *22*, 912−915.
(12) Brameld, K. A.; Kuhn, B.; Reuter, D. C.; Stahl, M. Small molecule conformational preferences derived from crystal structure data. A medicinal chemistry focused analysis. *J. Chem. Inf. Model.* **2008**, *48*, 1−24.
(13) Furet, P.; Caravatti, G.; Guagnano, V.; Lang, M.; Meyer, T.; Schoepfer, J. Entry into a new class of protein kinase inhibitors by pseudo ring design. *Bioorg. Med. Chem. Lett.* **2008**, *18*, 897−900.
(14) Zhang, G.; Ren, P.; Gray, N. S.; Sim, T.; Liu, Y.; Wang, X.; Che, J.; Tian, S.-S.; Sandberg, M. L.; Spalding, T. A.; Romeo, R.; Iskandar, M.; Chow, D.; Seidel, H. M.; Karanewsky, D. S.; He, Y. Discovery of pyrimidine benzimidazoles as Lck inhibitors: Part I. *Bioorg. Med. Chem. Lett.* **2008**, *18*, 5618−5621.
(15) Ohkubo, A.; Kasuya, R.; Miyata, K.; Tsunoda, H.; Seio, K.; Sekine, M. New thermolytic carbamoyl groups for the protection of nucleobases. *Org. Biomol. Chem.* **2009**, *7*, 687−694.
(16) Selected chemical stability data are shown in the Supporting Information.
(17) pK_a determination was performed at Sirius using the D-PAS technique.
(18) Testing against a large kinase panel was performed at Invitrogen. The data are shown in the Supporting Information.
(19) Wenglowsky, S.; Ahrendt, K. A.; Buckmelter, A. J.; Feng, B.; Gloor, S. L.; Gradl, S. N.; Grina, J.; Hansen, J. D.; Laird, E. R.; Lunghofer, P.; Mathieu, M.; Moreno, D.; Newhouse, B.; Ren, L.; Risom, T.; Rudolph, J.; Seo, J.; Sturgis, H. L.; Voegtli, W. C.; Wen, Z. Pyrazolopyridine inhibitors of B-Raf^{V600E}. Part 2: Structure−activity relationships. *Bioorg. Med. Chem. Lett.* **2011**, *21*, 5533−5537.
(20) Chu, K. A.; Yalkowsky, S. H. Predicting aqueous solubility: the role of crystallinity. *Curr. Drug Metab.* **2009**, *10*, 1184−1191.